Diffusion of trace elements in FeNi metal: application to zoned metal grains in chondrites

K. RIGHTER[1], A. J. CAMPBELL[2], M. HUMAYUN[2,*]

[1] Mail Code ST, NASA Johnson Space Center, 2101 NASA Pkwy., Houston, TX 77058

[2] Department of the Geophysical Sciences, The University of Chicago, 5734 S. Ellis Ave., Chicago, IL 60637

* Present address: Department of the Geological Sciences & National High Magnetic Field Laboratory, Florida State University, 1800 E Paul Dirac Drive, Tallahassee, FL 32310

submitted to Geochimica et Cosmochimica Acta, June 2004.

Revised and resubmitted, January 2005

Abstract

We have measured diffusion coefficients for P, Cr, Co, Ni, Cu, Ga, Ge, Ru, Pd, Ir and Au in Fe metal from 1150 to 1400 ˚C and at 1 bar and 10 kbar. Diffusion couples were prepared from high purity Fe metal and metal from the IIA iron meteorite Coahuila (single crystal kamacite) or the pallasite Springwater (polycrystalline kamacite), and held at run conditions for 3.5 to 123 hrs. Diffusion profiles were measured using laser ablation inductively coupled plasma mass spectrometry (LA-ICP-MS), or the electron microprobe. Many elements were measured from the same experimental runs so inter-elemental comparisons are improved over other data sets in which data for different elements come from different experiments. Some literature diffusion coefficients (D) for Ni and Co in taenite can be up to a factor of 3 higher for Ni than Co, yet our results show no difference (e.g., D_{Ni} and $D_{Co} \sim 2.2 \times 10^{-15}$ m^2/s at 1150 ˚C). Thus, diffusion of Ni and Co in single crystal taenite will not measurably fractionate the Ni/Co ratio. On the other hand, the large difference in D_{Ni} and D_{Ir} (D_{Ir} is ~5x lower) and the similarity of D_{Ni} and D_{Ru} at all temperatures investigated indicates that Ni/Ir and Ni/Ru ratios in zoned metal grains will be useful discriminators of processes controlled by diffusion versus volatility. In zoned metal grains in primitive chondrites, deviations of the Ni/Ru and Ni/Ir ratios from a condensation curve are opposite to a diffusion-controlled process, but consistent with a volatility-controlled process. The new multi-element diffusion coefficients will also be useful in evaluating a variety of other processes in planetary science.

Introduction

A thorough knowledge of diffusion of siderophile elements in planetary metals has many applications in cosmochronometry, redox processes, kamacite/taenite cooling rates, and the origin of zoned metal grains in chondrites. Hypotheses involving diffusional processes are difficult to evaluate for many elements due to lack of diffusion data for appropriate metal compositions, degrees of metal crystallinity, or relevant conditions for chondritic meteorites. Furthermore, what data exist can have a significant amount of variation between studies, making inter-elemental comparisons uncertain (Figure 1).

We have measured diffusion coefficients for Cr, Co, Ni, Ga, Ge, Ru, Pd, Ir, and Au in Fe metal : IIA iron meteorite metal couples from 1150 to 1400 ˚C, at both 1 bar and 10 kbar. We have also measured diffusion coefficients for P, As and Pt at a single temperature in several runs. These new measurements offer two advantages. First, the low concentrations of most siderophile elements in the meteoritic metal allow determination of diffusion coefficients at concentration levels appropriate for natural systems (Ni and Co are relatively high, but still at natural levels, ~6.0 wt% and ~0.5 wt%, respectively). Second, the results will provide an internally consistent data set in that diffusion coefficients for all elements were determined from the very same experiments, thus reflecting more realistic relative differences. The results are used to evaluate the role of diffusion in controlling the zoning in metal grains in metal-rich chondrites, and to illustrate the potential for diffusion to control the distribution and mobility of Cr, Ni and Ir in planetary metals.

Experimental

Diffusion couples were prepared from high purity Fe metal rod (Alfa Aesar 99.995% Fe, initially polycrystalline, and oriented with 110 plane coincident with diameter of rod) and metal from the IIA iron meteorite Coahuila (initially single crystal kamacite) or the pallasite Springwater (initially containing a micro-Widmanstätten pattern and kamacite outlining olivine). Starting materials were chosen to closely approximate natural Fe-Ni metals because diffusion coefficients are compositionally dependent, and the Fe-Ni alloys are the compositions of interest to cosmochemistry. Compositions of starting materials are given in Table 1. Metal lengths were lathed into rods and cut into 3 mm lengths (Fig. 2). The circular faces of these rods were polished and then the coupled rods were encapsulated with MgO. For 1 bar runs, the couples were first hot pressed for annealing for one hour at 10 kbar (in a piston cylinder apparatus) and at the same temperature as the target temperature for the run. The annealing was done to ensure physical contact between the two halves of the couple. One might question whether plastic strain occurred at these higher pressures during the anneal, and cause increased diffusion rates due to the introduction of dislocations. However, this is not relevant in this case for the following reasons: 1) the relatively long run times of the 1 bar experiments – all > 84 hours, compared to the one hour anneal time, 2) hydrostatic pressure does not cause permanent strain unless it is greater than the yield strength (Poirier, 1985), which did not occur in this case, and 3) plastic strain has potentially strong effects on anisotropic metals, but the metals here are isotropic (Poirier, 1985; Davidson et al., 1965). For the 10 kb runs, no hot pressing step was necessary. The MgO-sheathed metal couples (Fig. 2) were then placed either in a piston cylinder apparatus (10 kb) or alumina crucible within an evacuated silica tube (1 bar) in a vertical furnace, and held at run temperature (with

the duration depending upon the temperature; Table 2). In both experimental configurations, Fe is in contact with alumina. Therefore oxygen fugacity in the experiments was fixed near the IW buffer by equilibria between metal and alumina: Fe + Al_2O_3 + 1/2 O_2 = $FeAl_2O_4$ (e.g., Atlas and Sumida, 1958).

Run products were then mounted in epoxy, cut perpendicular to the interface and polished. In some cases, the crystallinity of samples was examined by etching a polished surface or by x-ray diffraction. In this way the grain size could be determined, and the issue of whether diffusion occurred through single crystals or a polycrystalline matrix could be evaluated. Both the Fe rod and the kamacite had changed structure to taenite under the run conditions. X-ray diffraction patterns of run products reveal both polycrystallinity and loss of 110 orientation in the pure Fe half of the couple. In experiment #6, a diffusion couple run at 10 kb, 1400 ˚C and one of the shortest runs in this study (19 hrs.), the grain size near the couple interface was large (150 to 300 μm), as defined by clear grain boundaries in the etched products. In longer runs such as experiments #19 or #20 (84 hrs.), grain boundaries are not evident, indicating that the annealing process has coarsened grain size even further. Diffusion profiles were thus acquired across single crystal interfaces. Additionally, when grain boundaries are crossed in a diffusion profile, there is typically a small peak within the profile (e.g., Dean and Goldstein, 1986, for phosphorus). We did not observe any such peaks in our profiles.

Analytical

Polished sections of the run products were examined using scanning electron microscopy (SEM). No phosphide rhabdites, sulfides, or chromites were observed in the

run products. Small MgO grains from the sample assembly occasionally occurred along the diffusion interface and were identified using the SEM and avoided because they could affect the diffusion process across the interface. In most cases the low, natural concentrations of siderophile elements were lower than the detection limits of electron microprobe analysis (~100 ppm). Diffusion profiles were measured using an electron microprobe for major elements (Ni, Co, P), and laser ablation inductively coupled plasma mass spectrometry (LA-ICP-MS) for trace elements (Fig. 3).

Iron, Ni, Co and P were analyzed with a CAMECA SX-50 electron microprobe at the University of Arizona, using an accelerating voltage of 15 kV and beam current of 20 nA. Standards include Fe, Ni, Co, and GaP and KOVAR metal (FeNiCo alloy). PAP phi-rho-z corrections were used in the data reduction (Pouchou and Pichoir, 1991).

Diffusion profiles for trace elements were measured using LA-ICP-MS. A CETAC LSX-200 laser ablation peripheral (Nd:YAG 266 nm) was used for solid sample introduction into a magnetic sector ICP-MS, the Finnigan Element, at the University of Chicago. Isotopes monitored were ^{59}Co, ^{60}Ni, ^{63}Cu, ^{69}Ga, ^{74}Ge, ^{75}As, ^{101}Ru, ^{105}Pd, ^{193}Ir, ^{195}Pt, and ^{197}Au. The laser spot size was 15 μm, and profiles were obtained using a scan rate of 5 μm/s. Mass sweeps were completed every approximately 0.75 s, and data points represent an average over several mass sweeps.

Instrumental sensitivity correction factors for each isotope were determined by measuring signal intensity from metal standards that have known concentrations of the elements of interest; these included the IVB iron meteorite Hoba, the IIA iron meteorite Filomena, and the NIST standard reference materials 1158 and 1263a (Campbell et al., 2001, 2002). Averages of at least 5 measurements from each standard were used in the

calibrations. The corrected intensities were converted to elemental abundances by normalization to [Fe] + [Co] + [Ni] = 100 wt%. Precision of the LA-ICP-MS measurements of PGE's was typically +/- 11 % (1□), based on repeat measurements of the Hoba standard. Counting statistics contributed a significant proportion (typically ~40%) to the variance. The suitability of the grain size and other aspects of iron meteorites for use as standards, as well as the precision and accuracy of analyses of a variety of trace elements in natural metals, have been discussed earlier (Campbell and Humayun, 1999; Campbell et al., 2002).

Results

Diffusion profiles for these experiments are defined both by electron microprobe analyses of Ni, Co or P, and by LA-ICP-MS analyses of trace metals such as Ru. The profiles obtained had constant composition at each end of the diffusion interface (Fig. 3), and the diffusion coefficients were derived assuming diffusion in a semi-infinite medium (Fig. 2). Diffusion (of element i) is governed by Fick's Second Law,

$$\left(\frac{\partial C_i}{\partial t}\right)_x = D_i \left(\frac{\partial^2 C_i}{\partial x^2}\right)_t \qquad (1)$$

(where D_i is the diffusion coefficient, C is concentration, x is position and t is time) for which there are many solutions (e.g., Crank, 1975; Brady, 1995). In the case of diffusion in a semi-infinite medium, the solution has the form:

$$\frac{C_i - C_0}{C_1 - C_0} = \frac{1}{2} erfc\left(\frac{x}{2\sqrt{D_i t}}\right) \qquad (2)$$

where C_i = the concentration at a given x and t, C_1 is the concentration at x<0 at t=0, and C_0 is the concentration at x>0 at t=0. C_1 and C_0 are obtained by averaging the values of

constant composition at each end of the diffusion couple. Diffusion coefficients are derived by plotting:

$$erfc^{-1}\left[2 * \left(\frac{C_i - C_0}{C_1 - C_0}\right)\right] \text{ vs. } \left(\frac{x}{2\sqrt{t}}\right), \quad (3)$$

and $D = 1/m^2$, where m is the slope, and fit only to the data defining the profile (Fig. 4). The inverse of the complementary error function, $erfc^{-1}$, was determined using a generalized power series solution from the application *Mathematica* (Wolfram Research, Inc.; functions.wolfram.com). The position of the Matano interface (or midplane), x = 0, therefore, was found as follows (Crank, 1975): for initial conditions of C_0 where x>0 and C_1 where x<0,

$$\int_0^{+\infty} (C - C_0)\,dx = \int_{-\infty}^{0} (C - C_i)\,dx.$$

The discussion that follows will be split into two parts. The first involves the compositional dependence of the diffusion coefficient for Ni and Co since these two elements are present at concentration levels higher than a trace impurity, and should strictly be treated as a case of inter-diffusion. The second part involves a discussion of all other elements, which are treated as tracer impurity diffusion since they are present at very low concentration levels.

Interdiffusion – Ni and Co

Because one side of the diffusion couples is pure Fe metal, and the Coahuila metal contains relatively high concentrations of Ni and Co, there might be compositional effects on the diffusion of these elements. Because the difference in composition is small (0 vs. 6 wt% for Ni and 0 vs. 0.5 wt% for Co), the effect is likely to be small, but the magnitude of the effect is nonetheless of interest for comparison to other studies. In

order to illustrate the magnitude of the compositional effect for Ni and Co, Boltzmann-Matano analysis was carried out on run #18, a diffusion couple run at 10 kb, 1150 ˚C and 123 hrs. Using the Boltzmann solution of Fick's second Law :

$$D = -\frac{1}{2t}\frac{\partial x}{\partial N_A}\int_{N_{A_1}}^{N_A} x dN_A$$

(where x is the position and N_A is the concentration of element A in the alloy) and the procedure outlined by Reed-Hill (1973), the diffusion coefficient was calculated for three different compositions (Fig. 5). The positive dependence of D(Ni) on the Ni content of the FeNi alloy is expected, based on previous work such as Goldstein et al. (1965). The minor effect here, over a small compositional range is noted. Because the focus of this study is on relative differences in D, this minor effect over a small compositional range will be ignored.

Tracer impurity diffusion

Based on the previous assessment, the small Ni compositional gradient will have only a minimal effect on the diffusion coefficient for Ni. The effect of the Ni gradient on the diffusion of all other low concentration elements will be insignificant as well. Furthermore, because the composition of the couples is fixed for the experiments, the diffusion of all other elements can be treated as tracer impurity diffusion. Because the composition of the couples is fixed, this study can focus on relative differences in diffusion coefficients, and lead to important distinctions in diffusion behavior between elements.

A summary of all diffusion coefficients determined in this study is presented in Table 2 and Figure 6, and split into the 1 bar and 10 kb experiments. There are four general

groups of elements based on their relative diffusion coefficients. Phosphorus exhibits the highest diffusion coefficient (Fig. 6b), whereas Cr, Cu, Ga, Ge, and Au have lower values. Nickel, Co, Pd and Ru all have intermediate values, while Ir has the lowest values, approximately a factor of 5 lower than Ni. These very general groupings will be useful when simultaneously examining zoning patterns of all of these elements in meteoritic metal. The dependence of diffusion coefficients upon temperature can be fit to an Arrhenius equation, $D = D_0 * \exp(\Delta H/RT)$, where D_0 is the pre-exponential factor, ΔH is the activation enthalpy, and R is the gas constant, 8.31441 J/mol.K. A plot of logD vs. 1/T yields a slope that corresponds to ΔH and an intercept that corresponds to D_0 (Table 3).

At both 1 bar and 10 kb, the elemental groupings and relative diffusivities are similar, and there are a few additional data for As and Pt indicating that these two elements are rapid and intermediate diffusers, respectively (Fig. 6). Although it is difficult to make a direct comparison because of different metal compositions (12.6% Ni in Springwater vs. 5.5% Ni in Coahuila; Table 1) and crystallinity, D_{Pt} is similar in magnitude to D_{Pd} and D_{Ni}, whereas D_{As} is higher than D_{Ga} and D_{Ge} and is probably similar to D_P.

Discussion

Comparison to previous work

The relative importance of diffusion in metals is illustrated by comparing diffusion data for Co in olivine (Morioka, 1980) and akermanite (Morioka and Nagasawa, 1991) to D(Co) in FeNi metal from this study (Table 2). Cobalt diffusion in taenite (from this study) is 100 x more rapid than Co diffusion in either olivine or akermanite (at a given

temperature). Thus, diffusion of siderophile elements in metals will be relatively rapid in mixed metal-silicate systems.

Nickel

Comparison can also be made to literature data for selected elements (Fig. 7). For instance, Goldstein et al. (1965) measured Ni diffusion coefficients in FeNi alloys and found that diffusion coefficients for Ni vary with Ni content; diffusion coefficients for Ni in $Fe_{90}Ni_{10}$ metal are approximately a factor of 15 lower than those in $Fe_{30}Ni_{70}$ metal. Our results for low Ni metal agree in general with this earlier work (Figure 7a); however, there is a significant difference in slope, or activation energy. A main contributing factor to the differences (in slope or ΔH) between this work and Goldstein et al. (1965) is the influence of phosphorus. Studies by Heyward and Goldstein (1973) and Dean and Goldstein (1986) have shown that diffusion of Ni in the ternary Fe-Ni-P system is faster than in the binary Fe-Ni, even with P contents as small as 0.25 wt%. The lower activation energy has been attributed to the effect of Group Va metals such as P, As and Sb, which increase vacancy density and therefore enhance diffusivity (Dean and Goldstein, 1986). Dean and Goldstein (1986) argued that P-bearing Fe-Ni metal would promote diffusion of many elements since the P acts to decrease the vacancy formation energies and thus increase the vacancy concentration. Since our couples have a small amount of P, the differences in activation energy (or slope) are likely due to P concentrations rather than Fe/Ni ratios.

Chromium, cobalt, palladium and ruthenium

Comparison of D(Cr), D(Co), D(Pd) and D(Ru) from the literature (e.g., compilation of Mehrer, 1995) illustrates the dangers of assembling data from various sources and

techniques to interpret relative elemental variations in natural samples. For instance, literature values for D(Cr) and D(Co) show large differences at a given temperature, yet our results show only a modest difference of approximately 4 (Fig. 7b). Furthermore, literature data for Ru and Pd would suggest similar diffusion coefficients at 1150˚C (Fig. 7c). However, our results show a clear and significant difference in their diffusion coefficients at temperatures <1250 ˚C (Fig. 7c). The shallower slope of D(Pd) vs. 1/T for our results compared to literature studies could also be due to the effect of phosphorus (Dean and Goldstein, 1986), as discussed above for D(Ni). Finally, measurements of D(Ru) in Ni-rich metal were made by Blum et al. (1989). Our results for D(Ru) across similar temperatures are nearly identical (Figure 7c), suggesting that Ni content has only a small effect on D(Ru) in the FeNi system.

Copper, gold and iridium

Comparison of D(Cu) to results of Watson and Watson (2003) indicates agreement at temperatures of overlap between the two studies. However, D(Pd) and D(Au) are lower by nearly an order of magnitude at all temperatures investigated in our study (Fig. 7d). Most of this difference is likely due to two effects. First the Ni content in our metal (5 to 6 wt%) is slightly lower compared to that in their study (10 wt%). Second, much of the difference could be due to differences in the concentrations of diffusing element. In contrast to the natural abundances employed in the present study, Watson and Watson (2003) used 1 to 2 wt% levels of siderophile elements in their diffusion couples. Higher doping levels are known in other systems to increase diffusivity (e.g., Ni in Goldstein et al., 1965). Finally, D(Ir) from our studies and previously reported D(Os) coefficients (Watson and Watson., 2001) show a similarly low relative value to D(Ni), indicating that

Ir and Os have relatively low diffusion coefficients, as might be expected given other similarities in their chemical properties (e.g., Shirey and Walker, 1997).

In summary, the absolute differences in D(Ru), D(Pd), D(Au), D(Co) and D(Cr) between the various studies and our work is most likely due to differences in metal composition and tracer impurity concentrations, but defect density and crystallinity, could also play a role. Measuring multiple elements in a single run improves inter-element comparisons and is one of the strengths of our approach and dataset.

Comparison to Stokes-Einstein equation estimates

The Stokes-Einstein equation is sometimes used to estimate diffusion coefficients in the absence of data. The Stokes-Einstein equation predicts that the diffusivity of i through medium j (D_{ij}), is inversely proportional to the atomic radius of the diffusing species, R_i according to: $D_{ij}\eta_j/\kappa T = 1/6\pi R_i$ (where η_j is viscosity, κ is Boltzmann constant, and T is temperature; Bird et al., 1960). However, our diffusion data show that this approach is not rigorous and would lead to erroneous values of D. Although there is an inverse correlation evident in a subset of elements such as Cr, Cu, Ge, Ru, Pd, and Ir, there are some glaring exceptions such as Ga, and Au, all of which have high D's but also large atomic radii (Fig. 8).

Comparison of diffusion coefficient and melting point temperature of the pure metal shows some correlation, as expected from diffusion theory (e.g., Shewmon, 1963). Although there are some trends with melting point, there are some notable exceptions such as Cr and Ga. In summary, Fig. 8, shows that there are no systematic trends of D with atomic radius, crystal structure, or melting point, demonstrating the advantage of measuring diffusion coefficients over theoretical predictions.

Effect of pressure

Our series of experiments at 10 kbar can be compared with our 1 bar data to make an assessment of the effect of pressure (Figure 9). There is approximately one order of magnitude decrease in D(Ni) between 1 bar and 10 kbar. This decrease is in accord with results of Goldstein et al. (1965) who showed a slightly larger decrease for D(Ni) in metal of composition $Fe_{90}Ni_{10}$, at 40 kbar (Figure 9a). Similarly, the values for D(Ga), D(Co), D(Ru) and D(Ir) are a factor of 3-10 higher at 1 bar than at 10 kbar, depending on the temperature of comparison (Table 2 and Fig. 9b). This is consistent with the results of Watson et al. (2003) who also showed a decrease in D(Pd) and D(Au) from 1 bar to pressures up to 200 kbar.

Origin of zoned metal grains in chondrites

Zoned metal grains have been found in several different chondrite groups, including CH chondrites and the Bencubbin-like group (e.g., Hammada al Hamra (HH) 237 and Queen Alexandra Range (QUE) 94411). The metal grains are zoned in major elements such as Fe, Ni, Co and P (Meibom et al., 1999; Weisberg et al., 1995; Campbell et al., 2001) as well as trace elements such as Mo, Cr, and the highly siderophile elements (HSE; Ru, Ir, Os, Rh, Pd, Pt, Re and Au) (Campbell et al., 2001). Refractory elements are enriched in the cores and depleted in the rims, and volatile elements such as Cr and P have a reversed zoning pattern with high concentrations at the rims. Several different origins of these striking grains have been proposed. Initial models proposed an origin by fractional condensation from solar nebular gas (e.g., Newsom and Drake, 1979; Weisberg

and Prinz, 1999; Meibom et al., 1999, 2001; Petaev et al., 2000, 2003). A second hypothesis, proposed by Campbell et al. (2001), is that the condensation of metal from a cooling gas would have to be in the presence of a gas saturated with refractory elements. Otherwise, the gas would be depleted in refractory siderophile elements early given their higher condensation temperatures, leading to super-enriched cores and depleted rims. A third hypothesis was proposed by Campbell et al. (2001) and followed on from the second scenario: early condensing metal grains have refractory siderophile element enriched cores and Fe-rich rims, and were later re-equilibrated by diffusional processes. Diffusion coefficients determined in this study can be used to place limits on the timescales of these hypotheses, especially since the diffusion behavior of the elements studied falls into several broad groups: fast (Cr, Cu, Au and P), intermediate (Ni, Co, Ru and Pd) and slow (Ir) diffusers.

Because Au, Cr, Cu and P commonly have flat or reverse profiles in grains that are otherwise zoned in Ni, Co, Ru, Rh, Os and Ir (Campbell and Humayun, 2004; Campbell et al., 2001), and these elements have higher diffusion coefficients than the latter (this study), these two groups of elements may provide information about the cooling rates and time required to preserve zoning in some grains but not others.

Diffusion coefficients reported by previous workers for Ni and Co in taenite are up to an order of magnitude different (Figure 1), yet they are always identical in experiments from this study. Some of the variation may be due to differences in crystallinity and grain size, experimental technique or metal composition. Some diffusion data reported in the literature is for polycrystalline metal, and any estimates of diffusion length scales utilizing such data will be overestimated. For example, the literature diffusion

coefficients for Ni and Co in taenite utilized by Meibom et al. (2001), are a factor of 3 higher for Ni than Co, yet our results show little difference (e.g., D_{Ni} and $D_{Co} \sim 2.2 \times 10^{-15}$ m^2/s at 1150 ˚C, using values from Table 3). This is also supported by the results of Badia and Vignes (1969) where D(Ni) and D(Co) are nearly identical in experiments at the same conditions for each element. Similarly, D_{Ni} and D_{Ru} are nearly the same (within a factor of 1.3 to 1.9) at all temperatures investigated indicating that Ni/Ru ratios will also not be fractionated strongly during diffusional re-equilibration (Figure 10). Thus, diffusion of Ni, Co and Ru in taenite will not strongly fractionate Ni/Co or Ni/Ru ratios (Figure 10).

On the other hand, the large difference in D_{Ni} and D_{Ir} (D_{Ir} is ~5x lower) at all temperatures investigated indicates that Ni/Ir ratios in zoned metal grains may be useful discriminators of whether diffusion has occurred (Figure 10). Because D_{Ni} is greater than D_{Ir} any diffusive re-equilibration of metal condensed from a solar nebular gas would produce a zoning pattern with relatively Ni-poor and Ir-rich metal (i.e., lower Ni/Ir ratios than initial).

Many CR, CH and CB chondrites contain unzoned as well as zoned metal grains, and if diffusional re-equilibration is involved in producing the unzoned grains, limits can be placed on the timescale of this process by considering the new diffusion data. Estimates of the timescale for diffusive re-equilibration can be made using a simple model for diffusion in a sphere (Crank, 1975). As a sphere with a concentration gradient from surface to center undergoes diffusive re-equilibration, Dt/a^2 (where t is time and a is radius) approaches 0.4 as the concentration profile is flattened or erased (Crank, 1975). By monitoring this value (Dt/a^2) during a cooling path, we can estimate how long a zoned

metal grain can exist under specific conditions, or how much time would be required to flatten a metal grain profile with an initially HSE-rich core. Using the new diffusion coefficients for Cr, Ni and Ir, representing fast, intermediate and slow diffusing elements in this study, the time required to eliminate a primary zoning pattern (from either hypothesis 1, 2 or 3 from above) during cooling of a taenite grain can be calculated. Assuming a 150 μm radius grain, with an initial temperature of 1373 K and a cooling rate of 0.011 + 0.022*ΔT K/hr. (based on the model of Petaev et al., 2003), and using the temperature dependence of 1 bar diffusion coefficients determined in this study (Table 2 and 3), Cr, Ni and Ir profiles will be flattened by diffusion in 75, 105 and > 115 days, respectively. For this calculation, Dt/a^2 is calculated at each step of the cooling path, and the times correspond to 50 steps (ΔT = 2 ˚C), 72 steps (ΔT = 10˚C), and >80 steps (ΔT = 20˚C), respectively. The value for Ir represents a lower limit because Ir diffuses so slowly – it is unlikely that Ir zoning patterns would be erased unless cooling was extremely slow. Two of the other fast diffusers, Ga and Au, both equilibrate faster than Cr on timescales of 25 to 40 days.

This demonstrates that whatever process was responsible for preserving the zoning patterns measured in QUE 94411 metal grains could have involved slow cooling for a short period time of time (< 100 days at ~0.01 K/hr) before a rapid temperature drop to preserve zoning in Ir and Ni. This is consistent with the calculations of Meibom et al. (2001), in which it is shown that metal grains of this size can grow in 84 hours or less. On the other hand, the production of unzoned metal grains documented in some meteorites (e.g., PCA91467 and ALH85085; Campbell and Hunayun, 2004) by a

diffusion-controlled process would require > 120 days along a slow cooling path to ensure no zoning of slow diffusing elements such as Ir or Os.

Future and conclusions

Zoning and composition of metal grains in chondrites can be caused by a number of different factors, such as growth rates, diffusion, re-equilibration with a gas, gas/dust ratios, and nebular pressures. The simple modelling in this contribution illustrates the important role defined by diffusional processes, but the zoned metal grains should be evaluated using a more detailed model that combines metal grain nucleation, condensation, growth, diffusion, and cooling histories similar to that of Petaev et al. (2003). In addition, generalized expressions relating temperature, pressure, and metal composition for diffusion coefficients would have a very widespread and useful application to many problems in meteoritics. However, too many gaps in the present experimental coverage of such parameters precludes the derivation of such expressions. Nonetheless, it is clear that these new data have placed constraints on the required timescales of diffusional equilibration and re-equilibration in producing zoned metal grains.

These new data will also be useful in evaluating a variety of processes in metal-bearing planetary materials such as isotopes and chronometry, redox processes, and kamacite/taenite based cooling rates. For instance, metal occurs in planetary materials in a variety of textures and grain sizes, such as small inclusions in chondrules (Grossman and Wasson, 1985), zoned metal grains (70 to 200 μm; Weisberg et al. 1995), lamellae in iron meteorites (Buchwald, 1975), metal chondrules (1 to 3 mm) in Bencubbin (Weisberg

et al., 1990), metal nodules in aubrites (cm sized; Casanova et al., 1993), metal veins in acapulcoites (McCoy et al., 1996) and metal-rich clasts in mesosiderites (up to 3 cm; Mittlefehldt et al., 1998). The time required for diffusional re-equilibration of metals in such materials can vary from less than a year (small grains) to hundreds of years (cm-sized metal clasts), at temperatures < 1100 ˚C, and up to millions of years for subsolidus equilibration (octahedrites).

Acknowledgements

We would like to thank T. McCoy of the Smithsonian Institution for providing samples of the Coahuila iron for use in the experiments. M.J. Drake provided access to his experimental facilities and supplies, supported by NSF grant EAR-0074036, and NASA grant NAGW-12795. Research was also supported by NASA grant NAG5-13133 to MH, as well as a NASA RTOP to KR. R. Downs and W. Bilodeau (Univ. of Arizona) kindly provided x-ray diffraction data on metallic run products and starting materials. Comments by H. Watson, J. Goldstein, W.F. McDonough, J. Wasson and M. Petaev were beneficial. We appreciate the review by A. Meibom. We thank J.Goldstein for a very thorough and constructive review.

References

Atlas, L.M. and Sumida, W.K. (1958) Solidus, subsolidus, and subdissociation phase equilibria in the system Fe-Al-O. *J. Amer. Ceram. Soc.* **41**, 150-160.

Badia, M. and Vignes, A. (1969) Diffusion in the Fe-Ni System. *Acta Metall.* **17**, 177-183.

Bird, R.B., Stewart, W.E., and Lightfoot, E.N. (1960) *Transport Phenomena*. John Wiley and Sons, New York, NY, 780 pp.

Blum, J.D., Wasserburg, G.J., Hutcheon, I.D., Beckett, J.R. and Stolper, E.M. (1989) Diffusion, phase equilibria and partitioning experiments in the Ni-Fe-Ru system. *Geochim. Cosmochim. Acta* **53**, 483-489.

Bowen, A.W. and Leak, G.M. (1970) Diffusion in bcc iron-base alloys. *Met. Trans.* **1**, 1695-1699.

Brady, J.B. (1995) Diffusion data for silicate minerals, glasses and liquids. in: T.J. Ahrens (ed.), *Mineral Physics and Crystallography: A Handbook of physical constants: AGU Reference Shelf volume 2*, American Geophysical Union, Washington, p. 269-290.

Buchwald, V. (1975) *Handbook of Iron Meteorites* (3 volumes). University of California Press, Berkeley, CA.

Campbell A. J. and Humayun M. (1999) Trace element microanalysis in iron meteorites by laser ablation ICPMS. *Anal. Chem.* **71**, 939-946.

Campbell, A.J.and Humayun, M. (2004) Formation of metal in the CH chondrites ALH85085 and PCA91467. *Geochim. Cosmochim. Acta* **68**, 3409-3422.

Campbell, A.J., Humayun, M. and Weisberg, M.K. (2002) Siderophile element constraints on the formation of metal in the metal-rich chondrites Bencubbin, Weatherford, and Gujba. *Geochim. Cosmochim. Acta* **66**, 647-660.

Campbell, A.J., Humayun, M., Meibom, A., Krot, A.N., and Keil, K. (2001) Origin of zoned metal grains in the QUE94411 chondrite. *Geochim. Cosmochim. Acta* **65**, 163-180.

Casanova, I., Keil, K. and Newsom, H. (1993) The composition of metal in aubrites: constraints on core formation. *Geochim. Cosmochim. Acta* **57**, 675-682.

Crank, J. (1975) The mathematics of diffusion. Oxford University Press, Oxford, UK, 414 pp.

Davidson, T.E., J.C. Uy, and A.P. Lee (1965) Hydrostatic pressure-induced plastic flow in polycrystalline metals. *Trans. Metall. Soc. AIME* **233**, 820-825.

Davis, A.M. (1977) The cosmochemical history of the pallasites. Ph.D. Thesis, Yale University, 285 pp.

Dean, D.C. and Goldstein, J.I. (1986) Determination of the interdiffusion coefficients in the Fe-Ni and Fe-Ni-P systems below 900 ˚C. *Met. Trans.*, **17A**, 1131-1140.

Fillon, J. and Calais, D. (1977) Self-diffusion in Fe-Pd alloys. *Jour. Phys. Chem. Solids* **38**, 81-89.

Goldstein, J.I., Hannemann, R.E. and Ogilvie, R.E. (1965) Diffusion in the Fe-Ni system at 1 atm and 40 kb pressure. *Trans. Met. Soc. AIME* **233**, 812-820.

Grossman, J.N. and Wasson, J.T. (1985) The origin and history of the metal and sulfide components of chondrules. *Geochim. Cosmochim. Acta* **49**, 925-939.

Henry, G., Barreau, G., and Cizeron, G. (1975) Coefficients of volume diffusion of Co in gamma Fe and in Fe-Co alloys. *Comptes Rendus Hebd. Seances Acad. Sci.* **280C**, 1007-1010.

Herzog, G.F., Flynn, G.J., Sutton, S.R., Delaney, J.S., Krot, A.N., Meibom, A. (2000) Low Ga and Ge contents in metal grains from the Bencubbin/CH-like meteorite QUE 94411 determined by synchrotron X-ray fluorescence. *Met. Planet. Sci.* **35**, A71.

Heyward, T.R. and Goldstein, J.I. (1973) Ternary diffusion in the alpha and gamma phases of the Fe-Ni-P System. *Met. Trans* **4**, 2335-2342.

Hirano, K. Cohen, M., Averbach, B.L. (1961) Diffusion of nickel into iron. *Acta Met.* **9**, 440-445.

Krot, A.N., Meibom, A., Weisberg, M.K. and Keil, K. (2002) The CR chondrite clan: implications for early solar system processes. *Met. Plan. Sci.* **37**, 1451-1490.

Majima, K. and Mitani, H. (1978) Lattice and grain boundary diffusion of copper in gamma –iron. *Trans. Jap. Inst. Metals* **19**, 663-668.

McCoy, T., Keil, K. Clayton, R.N., Mayeda, T.K., Bogard, D.D., Garrison, D.H., Huss, G.R., Hutcheon, I.D., Wieler, R. (1996) A petrologic, chemical, and isotopic study of Monument Draw and comparison with other acapulcoites: evidence for formation by incipient partial melting. *Geochim. Cosmochim. Acta* **60**, 2681-2708.

Mehrer, H. (1995) *Diffusion in solid metals and alloys*, volume 26, in Landolt-Bornstein Numerical data and functional relationships in Science and Technology. Group III: crystal and solid state physics. Springer-Verlag, New York.

Meibom, A., Petaev, M., Krot, A.N., Wood, J.A., and Keil, K. (1999) Primitive FeNi metal grains in CH carbonaceous chondrites formed by condensation from a gas of solar composition. *Jour. Geophys. Res.* **104**, 22053-22059.

Meibom, A., Desch, S.J., Krot, A.N., Cuzzi, J.N., Petaev, M.I., Wilson, L. and Keil, K. (2000) Large scale thermal events in the solar nebula: evidence from Fe,Ni metal grains in primitive meteorites. *Science* **288**, 839-841.

Meibom, A., Petaev, M., Krot, A.N., Keil, K. and Wood, J.A. (2001) Growth mechanism and additional condensation in the solar nebula. *Jour. Geophys. Res.* **106**, 32797-32801.

Mittlefehldt D.W., McCoy T.J., Goodrich C.A. and Kracher A. (1998) Non-chondritic meteorites from asteroidal bodies. In *Planetary Materials* (J.J. Papike, ed.) RIM **36**, 195 pp.

Morioka, M. (1980) Cation diffusion in olivine I. Cobalt and magnesium. *Geochim. Cosmochim. Acta* **44**, 759-762.

Morioka, M. and Nagasawa, H. (1991) Diffusion in single crystals of melilite: II. Cations. *Geochim. Cosmochim. Acta* **55**, 751-759.

Newsom, H. and Drake, M.J. (1979) The origin of metal clasts in the Bencubbin meteoritic breccia. *Geochim. Cosmochim. Acta* **43**, 689-707.

Petaev, M.I., Wood, J.A., Meibom, A., Krot, A.N. and Keil, K. (2000) The condensation origin of zoned metal grains in QUE94411: implications for the formation of the Bencubbin-like chondrites. *Met. Planet. Sci.* **36**, 93-106.

Petaev, M.I., Meibom, A., Krot, A.N., Wood, J.A, and Keil, K. (2003) The ZONMET thermodynamic and kinetic model of metal condensation. *Geochim. Cosmochim. Acta* **67**, 1737-1751.

Poirier, J.-P. (1985) *Creep of Crystals*. Cambridge Univ. Press, Cambridge, UK, 260 pp.

Pouchou, J.-L., Pichoir, F., 1991. Quantitative analysis of homogeneous or stratified microvolumes applying the model "PAP". In Heinrich, K.F.J. and Newbury, D.E. (Eds.), *Electron Microprobe Quantitation*. Plenum Press, New York, 31-75.

Reed-Hill, R.E. (1973) *Physical Metallurgy Principles*, PWS Kent Publishing Co., Boston, MA, 920 pp.

Rothman, S.J., Peterson, N.L., Walter, C.M., and Nowicki, L.J. (1968) The Diffusion of copper in iron. *Jour. Applied Phys.* **39**, 5041-5044.

Salje, G. and Feller-Kniepmeier, M. (1977) Diffusion and solubility of Cu in Fe. *Jour. Applied Phys.* **48**, 1833-1839.

Shewmon, P.G. (1963) *Diffusion in Solids*. McGraw-Hill, New York, NY, 205 pp.

Shirey, S. B. and R. J. Walker, 1997, The Re-Os isotope system in cosmochemistry and high-temperature geochemistry: *Ann. Rev. Earth Planet. Sci.* **26**, 423-500.

Watson, H.C. and Watson, E.B. (2003) Siderophile trace element diffusion in Fe-Ni alloys. *Physics Earth Planet. Int.* **139**, 65-75.

Watson, H.C., Fei, Y. and Watson, E.B. (2003) Diffusion of siderophile elements in iron-nickel alloys at high pressure and temperature. *Lunar Planet. Sci.* **XXXIV**, abstract 1871 [CD-ROM].

Watson, H.C. and Watson, E.B. (2001) Diffusion of siderophile elements in iron meteorites. American Geophysical Union, Fall Meeting 2001, abstract #V22A-1016.

Weisberg, M.K. and Prinz, M. (1999) Zoned metal in the CR clan chondrites. *Proc. NIPR Symp. Antarct. Meteorites* **24**, 187-189.

Weisberg, M.K., Prinz, M. and Nehru, C.E. (1990) The Bencubbin chondritic breccia and its relationship to CR chondrites and the ALH85085 chondrite. *Meteoritics* **25**, 269-279.

Weisberg, M.K., Prinz, M., Clayton, R.N., Mayeda, T.K., Grady, M., Pillinger, C.T. (1995) The CR chondrite clan. *Proc. NIPR Symp. Antarct. Meteorites* **8**, 11-32.

Figure Captions

Figure 1: Summary of diffusion data for Ni, Co and Cu in □Fe. The order of magnitude range of the data reflects the effects of various factors such as grain size and crystallinity (single crystal or polycrystalline), metal composition (purity), experimental technique (thin film, nuclear or diffusion couple), and analytical (electron microprobe, or other x-ray techniques). Data sources are as follows: Ni: Hirano et al., 1961; single crystal, thin layer residual activity method, Badia and Vignes, 1969; polycrystalline, diffusion couple and thin layer autoradiography; Mehrer, 1995, polycrystalline, thin layer residual activity; Co: Henry et al., 1975; polycrystalline, residual activity method; Badia and Vignes, 1969; polycrystalline, diffusion couple and thin layer autoradiography; Cu: Mehrer, 1995, polycrystalline, diffusion couple and EMPA, Rothman et al., 1968, single crystal, thin layer sectioning and counting, Salje and Feller-Kniepmeier, 1977, single crystal, thin layer and EMPA; Majima and Mitani, 1978, polycrystalline, thin layer residual activity method. The end points of temperature ranges covered in these studies are capped with a symbol.

Figure 2: A schematic diagram of the diffusion couple design used in these experiments. The two metal halves of the diffusion couple are enclosed by an MgO sleeve. The Coahuila (or Springwater) rod is always the top half of the couple.

Figure 3: Profiles of Ni (electron microprobe) and Ru (LA-ICP-MS) across the interface of experiment 15 and Ga (LA-ICP-MS) across experiment 18. Dashed lines are fits to the diffusion profiles using diffusion coefficients derived from equation (2) (see text). C_1 and C_0 are calculated as averages of the points on the "plateau" on each side of the profile. Vertical dashed lines are the Matano interface (defined in text).

Figure 4: Plot of $erfc^{-1}[2 * \frac{C_i - C_0}{C_1 - C_0}]$ vs. $\frac{x}{2\sqrt{t}}$ for experiments 15 and 18. All data are shown in A) and C), and only the linear portion of each profile for the fit is shown in B) and D). The diffusion coefficient is calculated from the inverse of the slope of the line squared, or D = $1/m^2$ (e.g., Crank, 1975). Vertical dashed lines are the Matano interface (defined in text).

Figure 5: Results of Boltzmann-Matano analysis for experiment #18, showing the effect of composition on D(Ni) and D(Co) for the small compositional range present in the couples comprised of Fe metal and Coahuila. Because the couples in this study have a fixed composition, and most elements are present at trace impurity levels (lower concentrations than Co), compositional effects are not significant.

Figure 6A: Summary of all 1 bar diffusion data from this study. **Figure 6B:** Summary of 10 kb diffusion data from this study. Note the presence of four general groups of elements – (P and As), (Cr, Cu, Ga, Ge, and Au), (Pd, Ni, Co, Pt and Ru), and (Ir). Errors bars are not included for each element due to the close spacing of many of the data points. However, all errors are presented in Table 2. Also note that all results from experiment #4 are not plotted in this diagram because the relatively Ni-rich Springwater metal makes a direct comparison more difficult; only the results for Pt and As are shown, and they are offset to the right on the 1/T axis for clarity (the experiment was carried out at 1400 ˚C).

Figure 7: A comparison of diffusion data from this study to previous work, including A) D(Ni) in FeNi metal at several different Fe:Ni ratios (Goldstein, et al., 1965), as well as the ternary Fe-Ni-P system with 0.25 wt% P (Heyward and Goldstein, 1973); B) D(Co) and D(Cr), from Henry et al. (1975) and Bowen and Leak (1970); C) D(Ru) and D(Pd)

from Blum et al., (1989) and Fillon and Calais (1977); and D) D(Cu), D(Au) and D(Pd) from Watson and Watson (2003). Our data are shown as solid symbols (Table 2) and fits to our data are from the relations summarized in Table 3. Data sources are as follows: Ni: Goldstein et al.,1965; polycrystalline, EMPA, Heyward and Goldstein, 1973; polycrystalline, diffusion couple method and EMPA; Co: Henry et al., 1975; polycrystalline, residual activity method; Cr: Bowen and Leak, 1970,; polycrystalline, residual activity method. Pd: Fillon and Calais, 1977; polycrystalline, steady state method. Ru: Blum et al., 1989; polycrystalline, thin layer method. Cu, Pd and Au: Watson and Watson, 2003; polycrystalline, diffusion couple method and EMPA). The end points of temperature ranges covered in previous studies are capped with a symbol.

Figure 8A: Comparison of D vs. atomic radius for 1 bar experiment at 1350 ˚C (expt. #15). An inverse correlation between D and atomic radii is predicted by the Stokes-Einstein equation, but is not evident in our data. Also shown are the structures of the various metals; there are no systematic trends with metal structure either. **Figure 8B:** Comparison of D vs. T/T_m (melting point temperature of the pure metal) for expt. #15. Although there are some trends with melting point, there are some notable exceptions such as Cr and Ga.

Figure 9A: D(Ni) from 1 bar and 10 kbar from this study compared to data of Goldstein et al. (1965) in $Fe_{90}Ni_{10}$ at 1 bar and 40 kbar. Although there is a slight difference in slope between the two studies, perhaps due to the presence of P in our experimental metals, there is general agreement in the magnitude of the pressure effect. **Figure 9B:** effect of pressure on D(Cr), D(Co), D(Ru) and D(Ir) at 1200, 1300 and 1400 ˚C. D

values for 1 bar normalizations were calculated using Arrhenius equations and constants from Table 3. Note the largest effect is at lower temperatures (1200 ˚C).

Figure 10A: Ni and Co in a core to rim zoned metal grain from Campbell et al. (2001), and the minimal effect of diffusion on Ni and Co contents when D(Ni) = D(Co). **Figure 10B:** The similarity in D(Ni) and D(Ru) also results in no change of this ratio during diffusional processes. **Figure 10C:** The factor of 5 difference between D(Ni) and D(Ir) should result in a greater change of Ni compared to Ir in zoned metal grains. Data from QUE94411 zoned metal grain is from Campbell et al. (2001).

Table 1: Composition of starting materials and zoned metal grains (in ppm)

Element (ppm)	Coahuila IIA iron	Springwater pallasite¥	Fe metal†	*QUE 94411 core§*	*QUE 94411 rim§*
P	2800	-	1.3	1200	3100
Cr	40	-	1.9	1500	2100
Co	4590	5950	8.3	4600	3200
Ni	55100	126000	2.9	59000	122000
Cu	140	153	1.5	-	-
Ga	57.6	19.2	0.37	<4	<4
Ge	178	32.4	1.7	<4	<4
As	-	27.8	0.08	-	-
Ru	23.4	0.82	< 0.005	3.7	12.4
Pd	1.81	6.25	< 0.01	3.3	3.8
Ir	18.17	61.0	< 0.01	2.8	6.9
Pt	31.77	1.58	< 0.01	4.9	11.7
Au	0.76	2.78	< 0.05	-	-
C	100	n.a.	0.0015	n.a.	n.a.
S	20	n.a.	3.5	n.a.	n.a.

§ from Campbell et al. 2001 and Herzog et al., 2000; ¥ Davis, 1977; † provided by Alfa Aesar; C and S data for Coahuila from compilation of Buchwald, 1975

Table 2: Summary of experimental run conditions and diffusion coefficients (m^2/s)

Expt. #	18	20	17	19	15	4	6	11	10	14
pressure	1 bar	1 bar	1 bar	1 bar	1 bar	10 kbar	10 kbar	10 kbar	10 kbar	10 kbar
temperature (˚C)	1150	1200	1255	1300	1350	1400	1400	1300	1200	1250
duration (hrs)	123	84	84	84	90	3.5	19	76	72	12
couple	Coahuila	Coahuila	Coahuila	Coahuila	Coahuila	Springwater	Coahuila	Coahuila	Coahuila	Coahuila
P	-	-	-	-	-	-	-	-	-	5.72(0.25)E-14
Cr	3.58 (4.3)E-15	6.80(1.30)E-14	1.96(2.2)E-14	4.15(2.0)E-14	6.03(1.0)E-14	-	-	-	5.72(1.45)E-16	-
Co	2.29(0.70)E-15	5.03(0.80)E-15	6.94(1.00)E-15	1.71(0.25)E-14	2.52(0.17)E-14	1.55(0.40)E-14	-	4.85(0.50)E-15	7.42(0.44)E-16	-
Ni	2.20(0.70)E-15	4.82(1.00)E-15	7.30(1.2)E-15	1.82(0.45)E-14	2.76(0.55)E-14	1.57(0.17)E-14	1.12(0.15)E-14	2.68(0.55)E-15	8.07(0.70)E-16	-
Cu	1.19(0.40)E-14	1.82(0.90)E-14	3.60(1.25)E-14	5.93(1.22)E-14	7.24(1.03)E-14	9.64(0.11)E-14	-	2.29(0.30)E-14	1.15(0.14)E-15	-
Ga	9.07(0.09)E-15	-	3.67(0.60)E-14	-	1.10(0.20)E-13	3.08(0.90)E-14	4.25(0.25)E-14	7.85(1.40)E-15	1.39(0.16)E-15	-
Ge	9.77(0.15)E-15	-	4.49(0.55)E-14	-	1.26(0.12)E-13	1.25(0.32)E-14	4.77(0.30)E-14	8.63(0.90)E-15	1.75(0.25)E-15	-
As	-	-	-	-	-	1.63(0.26)E-13	-	-	-	-
Ru	1.37(0.30)E-15	2.86(0.60)E-15	5.18(2.05)E-15	1.24(0.28)E-14	1.88(0.28)E-14	1.07(0.80)E-14	6.72(0.75)E-15	1.65(1.10)E-15	4.79(0.50)E-16	-
Pd	2.99(1.20)E-15	5.57(0.52)E-15	5.92(0.35)E-15	1.34(0.60)E-14	1.77(1.35)E-14	2.07(0.32)E-14	1.56(0.50)E-14	6.01(1.60)E-15	1.04(1.35)E-16	-
Ir	5.42(2.80)E-16	8.07(0.27)E-16	9.50(0.58)E-16	2.03(0.65)E-15	3.09(0.60)E-15	-	2.05(0.50)E-15	7.85(0.95)E-16	3.15(0.44)E-16	-
Pt	-	-	-	-	-	8.41(0.35)E-15	-	-	-	-
Au	5.83(0.35)E-15	1.20(0.60)E-14	2.08(1.50)E-14	5.19(2.60)E-14	8.60(0.45)E-14	2.83(0.50)E-14	1.47(0.23)E-14	-	1.25(0.80)E-15	-

1 error is shown in parentheses and is based on linear fits as in Fig. 4

Table 3: Diffusion constants (D_0) and activation energies (H) for 1 bar diffusion.

element	D_0 (m^2/s)	error	H (kj/mole)	error
Cr	$1.22 *10^{-4}$	$1.5 *10^{-5}$	-287	50
Co	$7.19 *10^{-7}$	$2.3 *10^{-8}$	-231	40
Ni	$2.25*10^{-6}$	$1.1 *10^{-7}$	-245	35
Cu	$7.11 *10^{-8}$	$1.5 *10^{-9}$	-185	35
Ga	$5.92 *10^{-6}$	$1.3 *10^{-7}$	-240	48
Ge	$1.12 *10^{-5}$	$0.6 *10^{-6}$	-246	66
Ru	$3.92 *10^{-6}$	$1.2 *10^{-7}$	-258	28
Pd	$5.24 *10^{-9}$	$1.5 *10^{-10}$	-170	53
Ir	$7.45*10^{-10}$	$2.5 *10^{-11}$	-168	44
Au	$2.48 *10^{-5}$	$1.0 *10^{-6}$	-263	31

Error cited is based on 90% confidence limits for the calculated coefficients

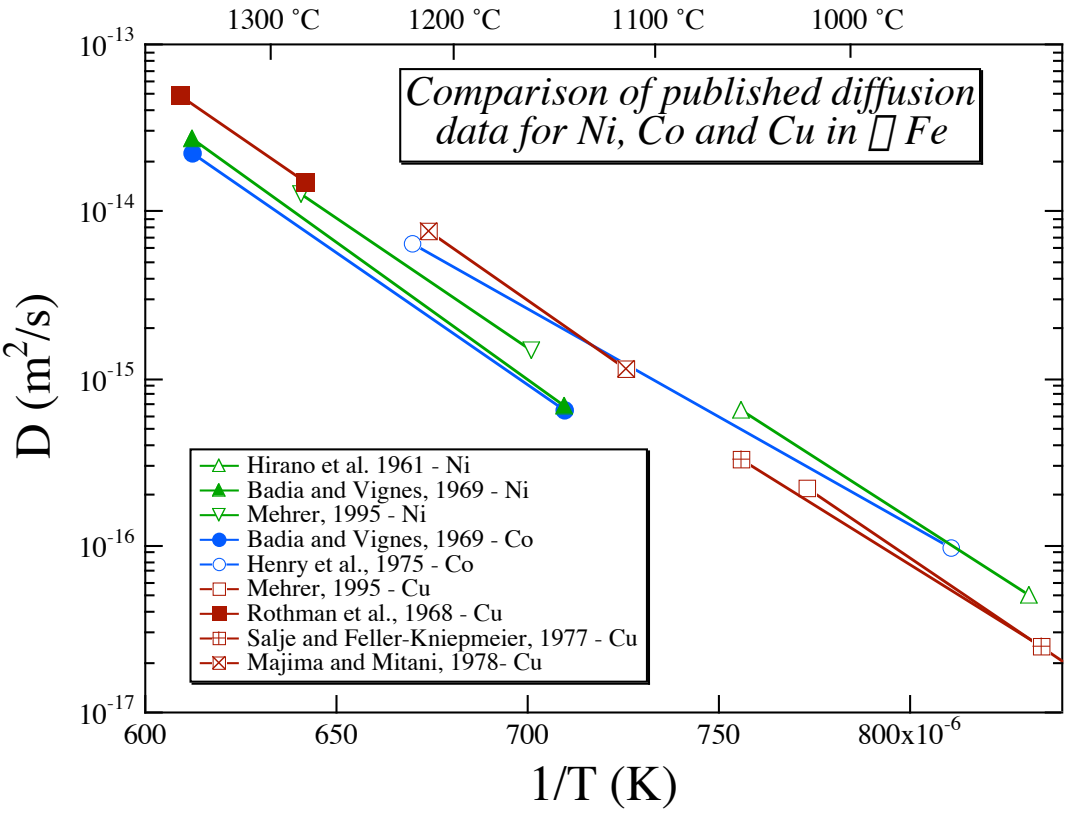

Fig. 1: Righter et al.

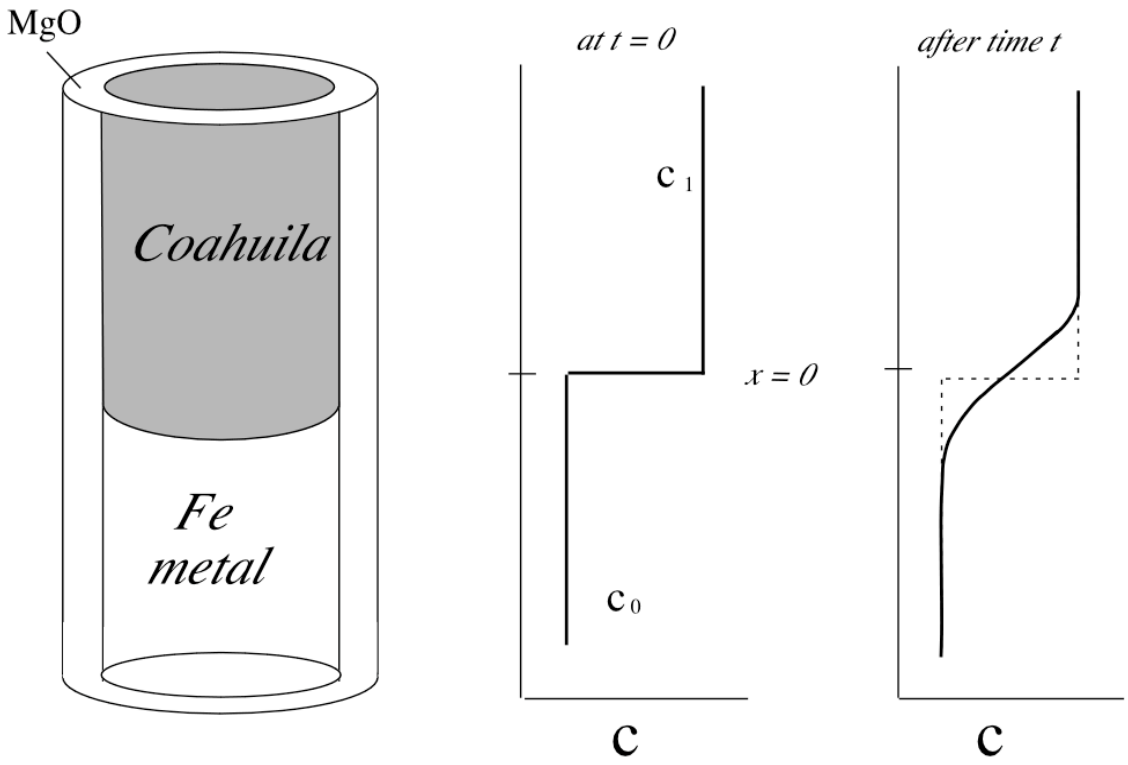

Fig. 2: Righter et al.

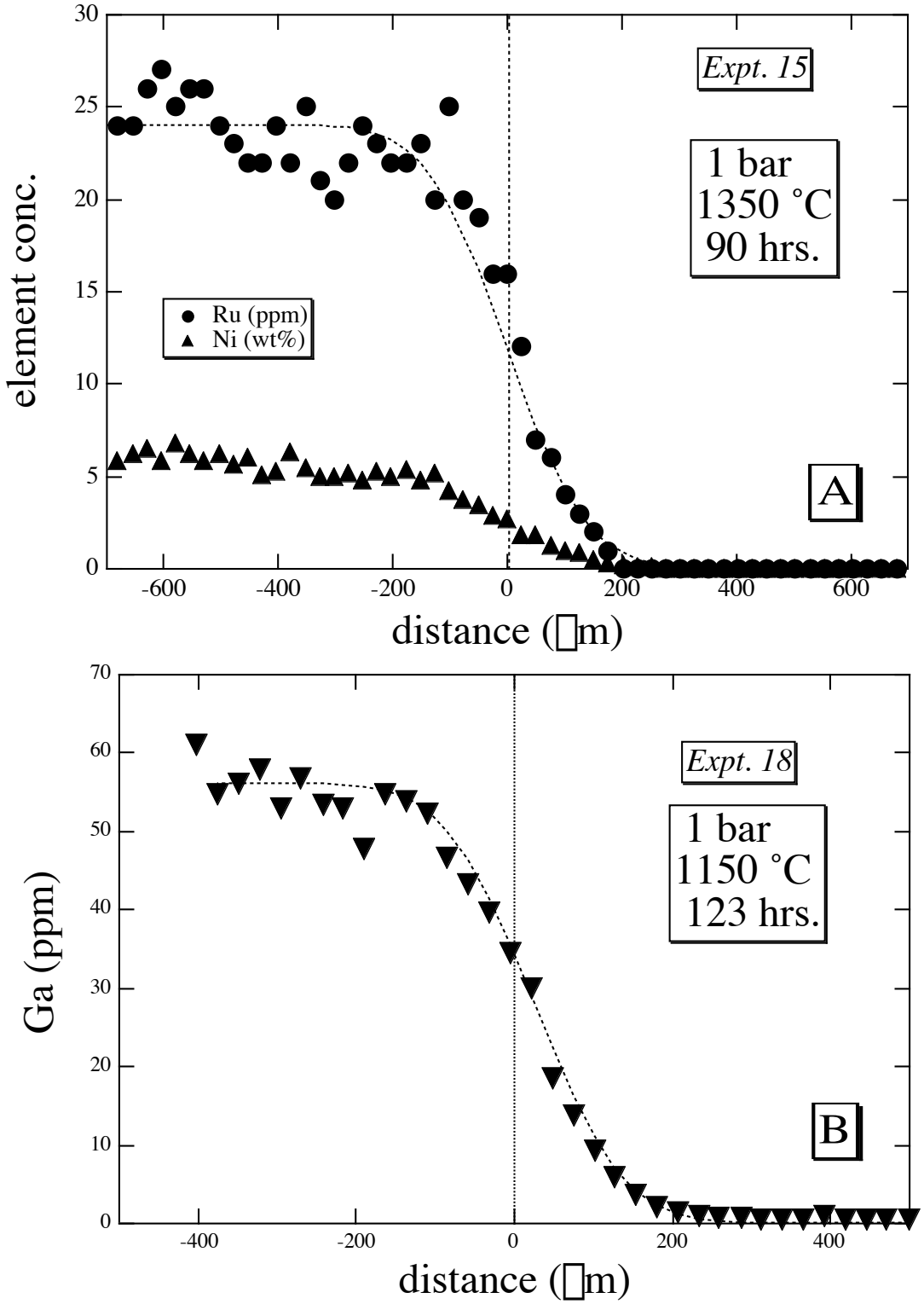

Fig. 3: Righter et al.

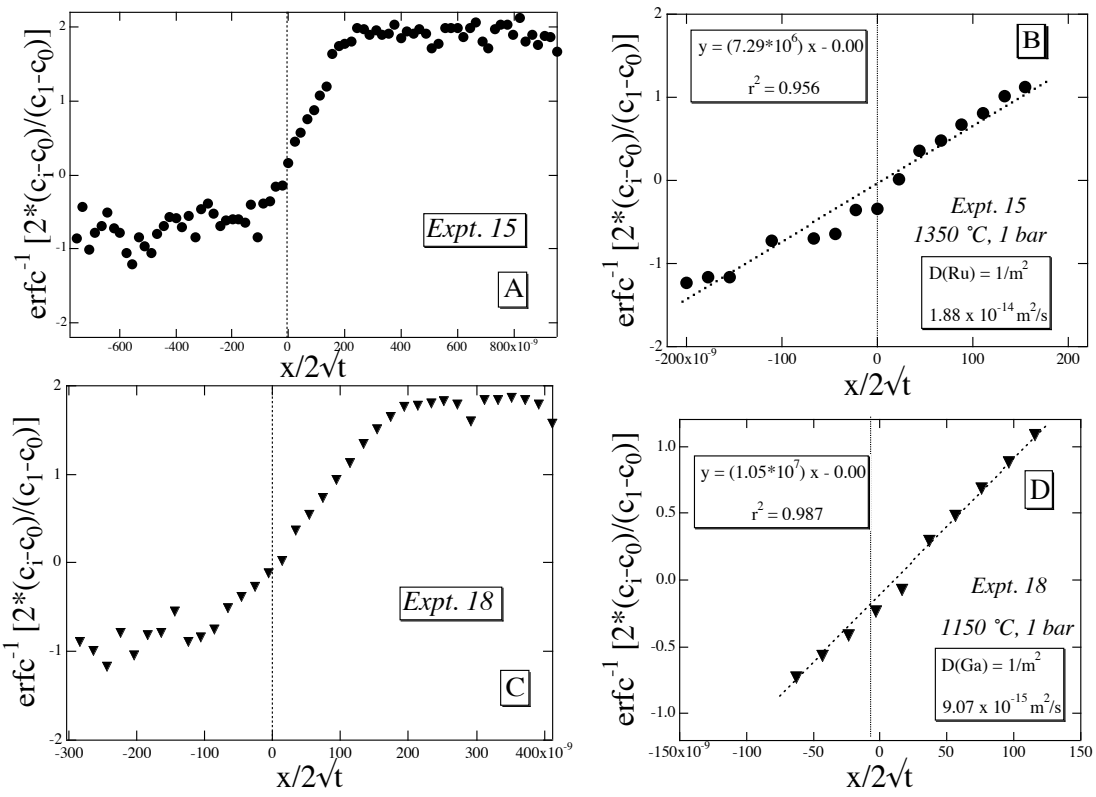

Fig. 4: Righter et al.

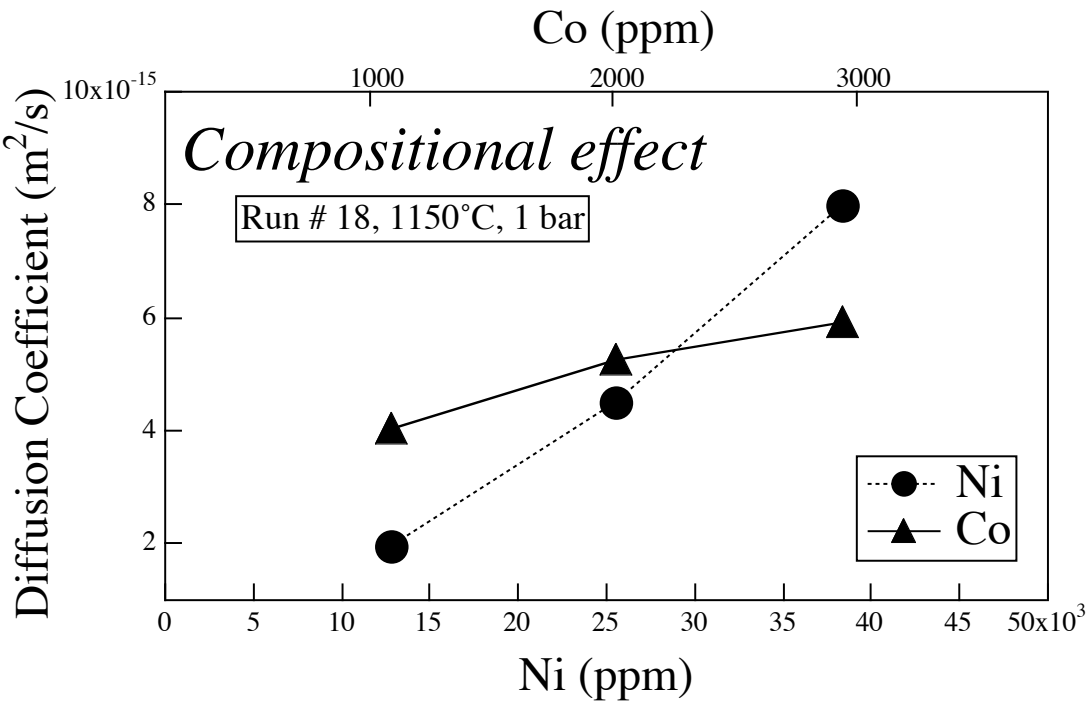

Fig. 5: Righter et al.

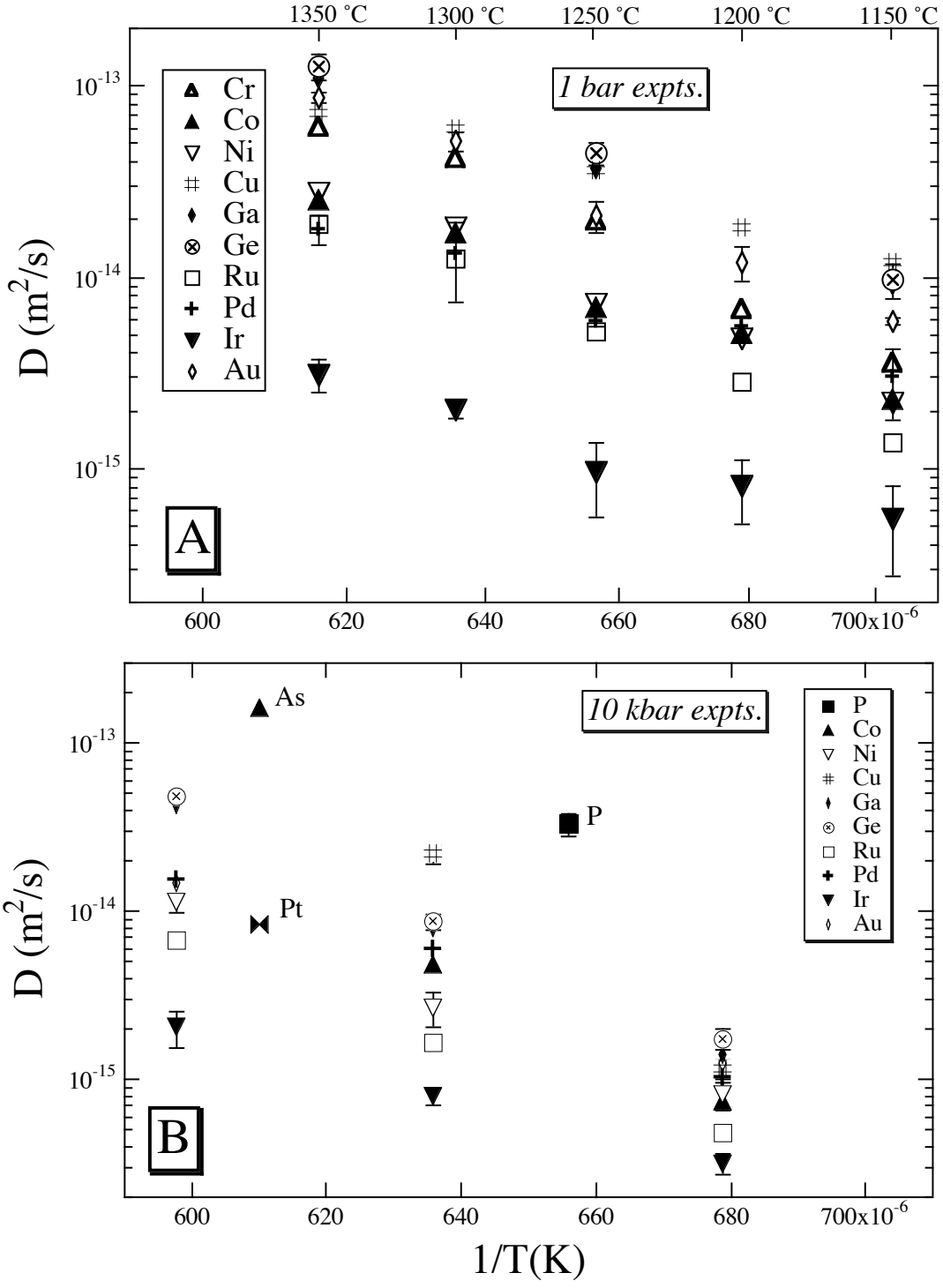

Fig. 6: Righter et al.

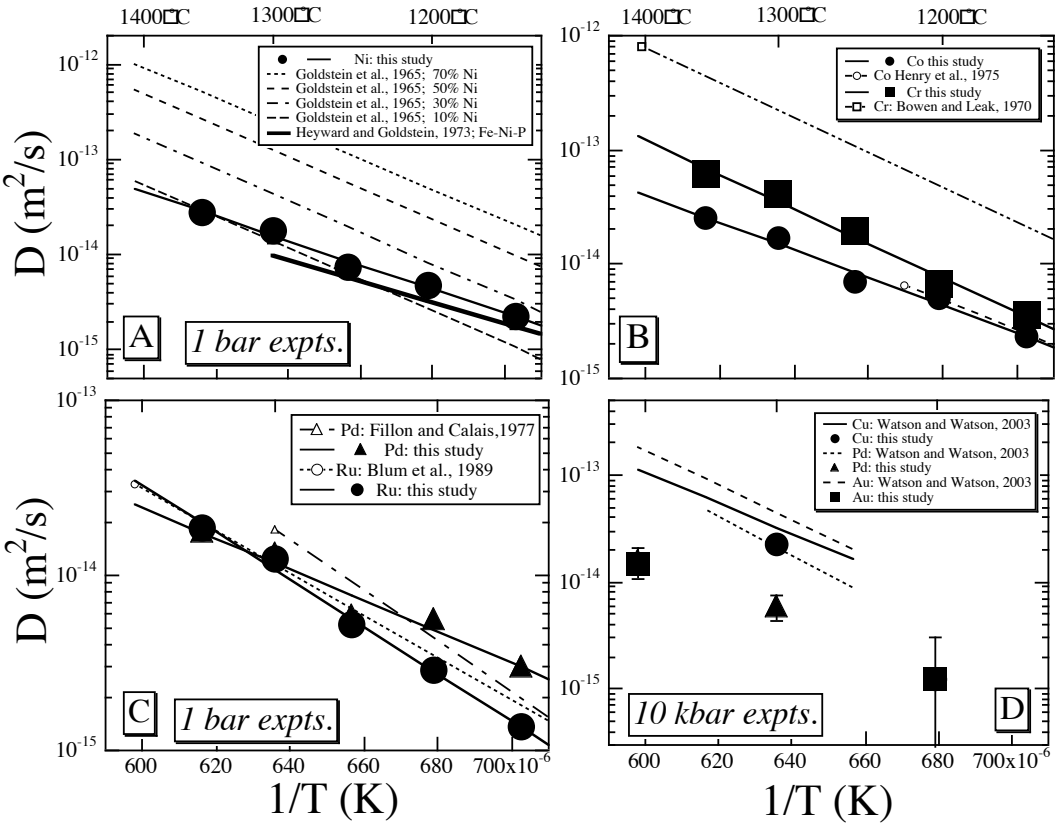

Fig. 7: Righter et al.

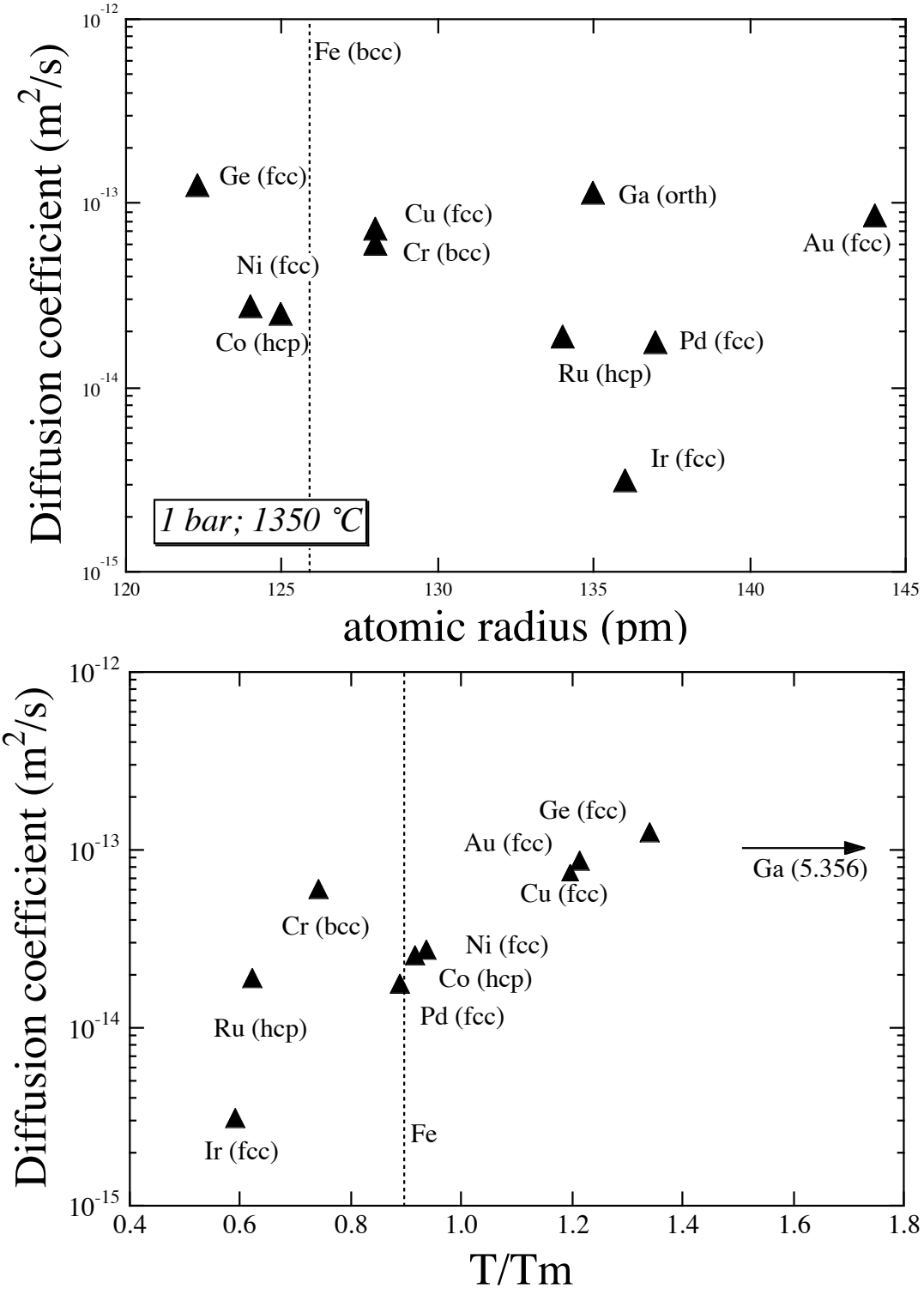

Fig. 8: Righter et al.

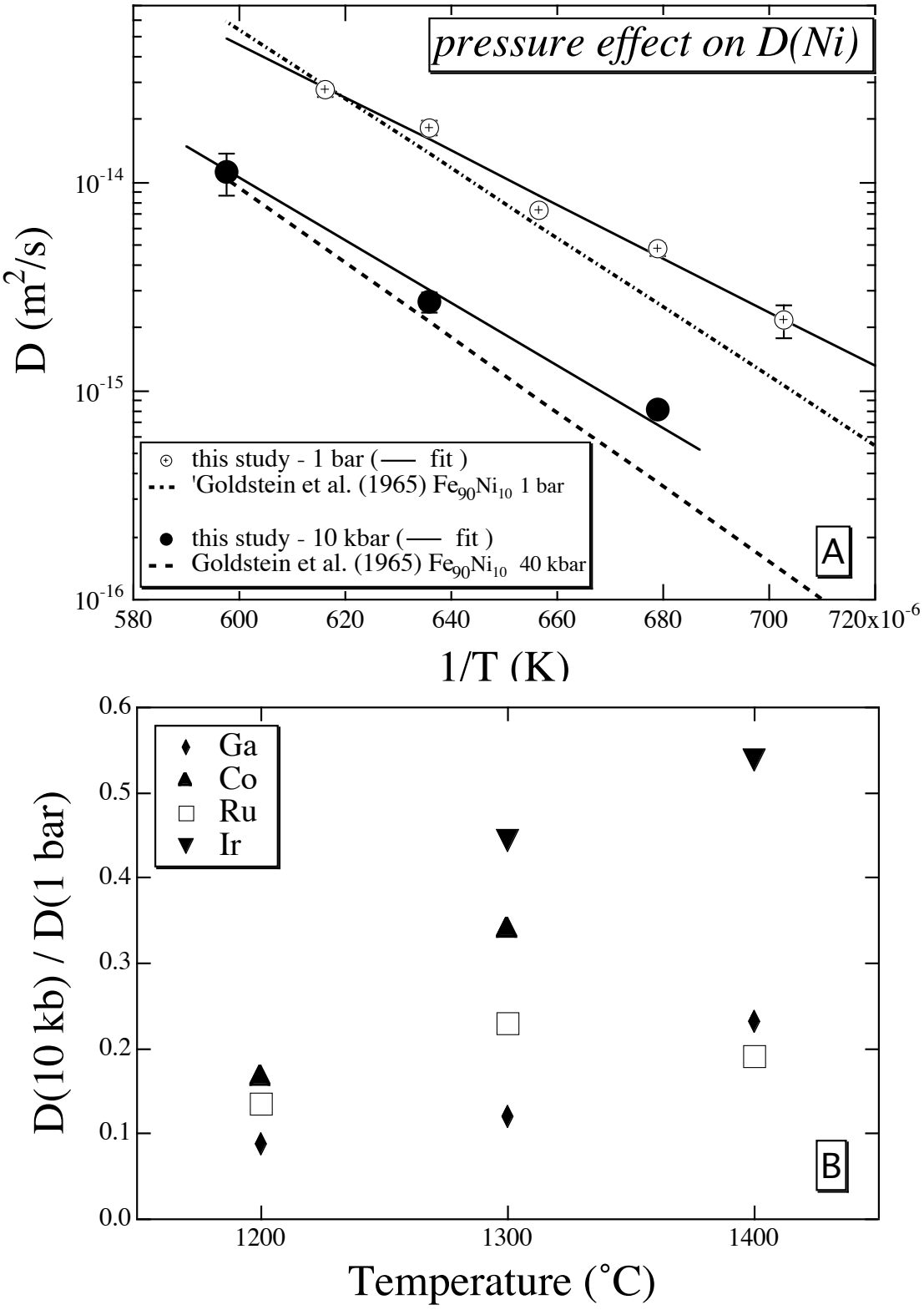

Fig. 9: Righter et al.

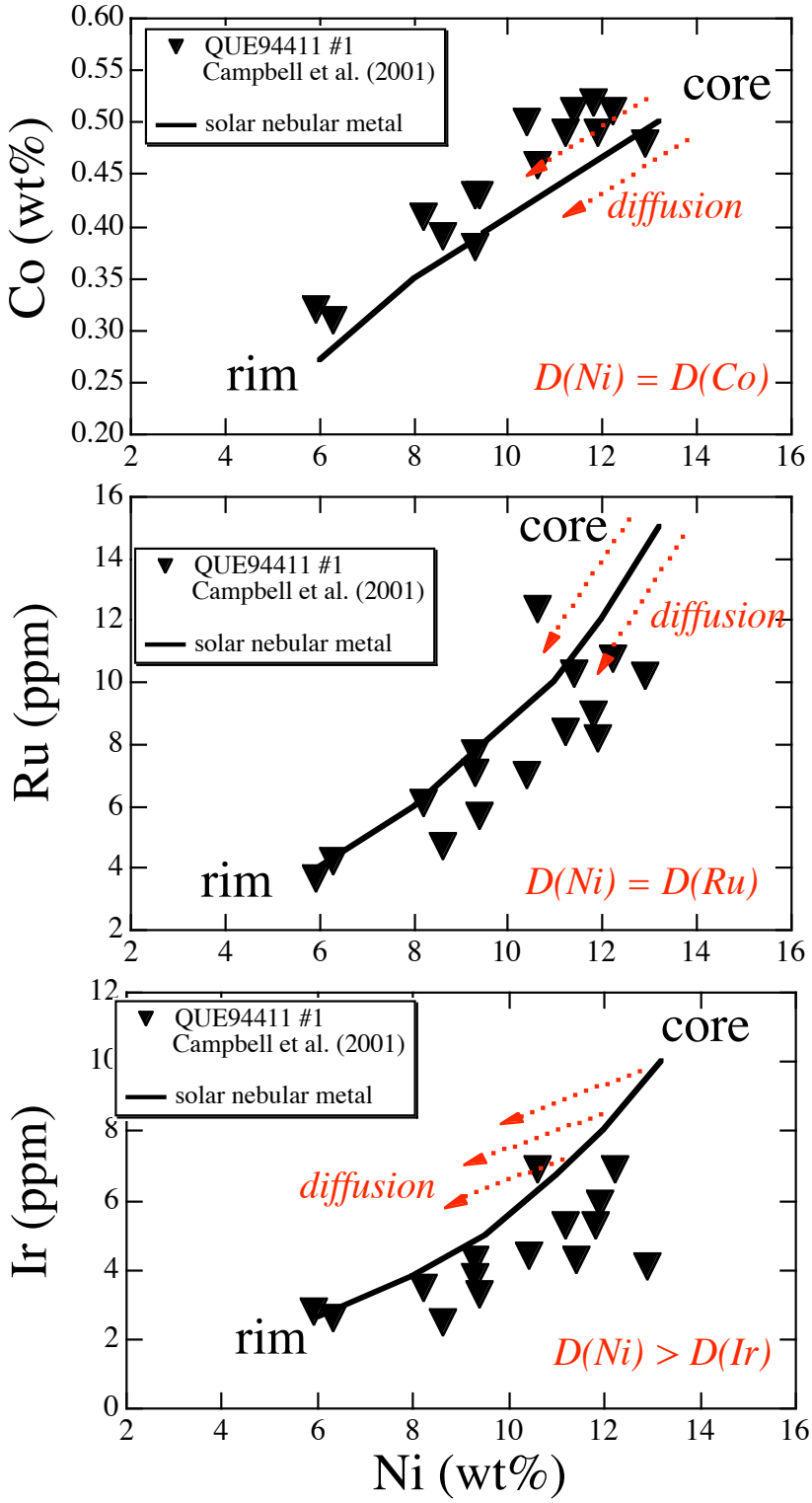

Fig. 10: Righter et al.